THYROID
Volume 33, Number 2, 2023

DOI: 10.1089/thy.2022.0336

Morphological and Functional Colonic Defects Caused by a Mutated Thyroid Hormone Receptor α

Minjun Kim,[1] Michael Kruhlak,[2] Victoria Hoffmann,[3] Patricia Zerfas,[3] Kevin Bishop,[4] Woo Kyung Lee Doolittle,[1] Elijah F. Edmondson,[5] Yuelin Jack Zhu,[2] and Sheue-yann Cheng[1]

Background: Mutations of thyroid hormone receptor α (TRα1) result in resistance to thyroid hormone (RTHα), exhibiting symptoms of retarded growth, delayed bone maturation, anemia, and severe constipation. Using a mouse model of RTHα (*Thra1*$^{PV/+}$ mouse), we aimed at understanding the molecular basis underlying the severe constipation observed in patients.
Methods: The *Thra1*$^{PV/+}$ mouse expresses a strong dominant negative mutant, PV, which has lost T3 binding and transcription activity. *Thra1*$^{PV/+}$ mouse faithfully reproduces growth abnormalities and anemia as shown in RTHα patients and therefore is a valid model to examine causes of severe constipation in patients. We used histopathological analysis, confocal fluorescence imaging, transmission electron microscopy (TEM), and gene expression profiles to comprehensively analyze the colonic abnormalities of *Thra1*$^{PV/+}$ mouse.
Results: We found a significant increase in colonic transit time and decrease stool water content in *Thra1*$^{PV/+}$ mouse, mimicking constipation as found in patients. Histopathological analysis showed expanded lamina propria filled with interstitium fluid between crypt columns, enlarged muscularis mucosa, and increased content of collagen in expanded submucosa. The TEM analysis revealed shorter muscle fibers with wider gap junctions between muscle cells, fewer caveolae, and hypoplastic interstitial cells of Cajal (ICC) in the rectal smooth muscles of *Thra1*$^{PV/+}$ mice. These abnormal histological manifestations suggested defective intercellular transfer of small molecules, electrolytes, and signals for communication among muscles cells, validated by Lucifer Yellow transferring assays. Expression of key smooth muscle contractility regulators, such as calmodulin, myosin light-chain kinase, and phosphorylated myosin light chain, was markedly lower, and c-KIT signaling in ICC was attenuated, resulting in decreased contractility of the rectal smooth muscles of *Thra1*$^{PV/+}$ mice. Collectively, these abnormal histopathological alterations and diminished contractility regulators led to the constipation exhibited in patients.
Conclusions: This is the first demonstration that TRα1 mutants could act to cause abnormal rectum smooth muscle organization, defects in intercellular exchange of small molecules, and decreased expression of contractility regulators to weaken the contractility of rectal smooth muscles. These findings provide new insights into the molecular basis underlying constipation found in RTHα patients.

Keywords: constipation, contractility, smooth muscles, thyroid hormone resistance, TRα mutations, transmission electron microscopy

[1]Laboratory of Molecular Biology, National Cancer Institute, National Institutes of Health, Bethesda, Maryland, USA.
[2]Laboratory of Cancer Biology and Genetics, National Cancer Institute, National Institutes of Health, Bethesda, Maryland, USA.
[3]Office of Research Services, Diagnostic and Research Services Branch, National Cancer Institute, National Institutes of Health, Bethesda, Maryland, USA.
[4]Translational and Functional Genomics Branch, National Human Genome Research, National Cancer Institute, National Institutes of Health, Bethesda, Maryland, USA.
[5]Molecular Histopathology Laboratory, Leidos Biomedical Research, Inc., Frederick National Laboratory for Cancer Research, Frederick, Maryland, USA.

Introduction

Thyroid hormone receptors (TRs) are critical in mediating the genomic actions of thyroid hormone (T3) in growth, development, and differentiation. Mutations of the *THRA* gene cause resistance to thyroid hormone (RTHα).[1,2] RTHα patients are characterized by nearly normal thyroid hormone and thyrotropin levels, but they exhibit growth retardation, delayed bone development, anemia, and constipation.[1–6] The molecular actions of TRα1 mutants in the bone abnormalities, erythroid disorders, and intestine defects have been studied in the *Thra1*$^{PV/+}$ mouse, a model of RTHα.

As found in RTHα patients, *Thra1*$^{PV/+}$ mice display growth retardation, have abnormal bone development,[7–9] exhibit anemia,[10,11] and cause epithelial defects in the adult intestine.[12] Collectively, these studies show that the *Thra1*$^{PV/+}$ mouse is suitable for further study of other pathological manifestations in patients.

When RTHα patients were first reported, one prominent symptom was severe constipation. Although intestinal defects in *Thra1*$^{PV/+}$ mice were reported,[12] it remained unclear how TRα1 mutations altered the activity of the colon, leading to severe constipation. Here, we show that *Thra1*$^{PV/+}$ mice exhibit constipation, as evidenced by increased colonic transit time, loss of water content in the stools, and extended colon length. The rectum of *Thra1*$^{PV/+}$ mice had abnormal morphological features in the lamina propria, muscularis mucosae, and submucosa.

Transmission electron microscopy (TEM) revealed markedly wider gap-junctions in the smooth muscle cells that impeded intercellular transfer of small molecules. The TEM analysis also showed hypoplastic and reduced number of interstitial cells of Cajal (ICC) to reduce smooth muscle contractility. We further detected decreased expression of key contractility regulators in the rectum of *Thra1*$^{PV/+}$ mice. Together, these defects result in impedance of the contractility of smooth muscles to understands how TRα1 mutations act, leading to constipation in RTHα patients.

Materials and Methods

Animals and treatment

All animal studies were performed according to the approved protocols of the National Cancer Institute Animal Care and Use Committee. Generation of *Thra1*$^{PV/+}$ mice was previously described.[13] All mice were fed with NIH 31 autoclavable Teklad laboratory animal diets from Envigo (Indianapolis, IN, USA). Further details are described in Supplementary Information.

Transmission electron microscopy

Female wild-type (WT) and *Thra1*$^{PV/+}$ mutant mice were used for TEM analysis (mouse age: ~7.2 months). Mouse colons of ~1 mm^3 were fixed for a minimum of 48 hours at 4°C in 2.5% glutaraldehyde and 1% paraformaldehyde in 0.1 M cacodylate buffer (pH 7.4). The subsequent steps were treated similarly as reported.[14]

Isolation of smooth muscle cells from rectum of mice

Rectum was dissected from euthanized female mice WT and mutant mice, aged ~7.4 months from which smooth muscle cells were isolated as previously described.[15]

Lucifer Yellow dye transfer assay

Lucifer Yellow (150 mM) solution prepared as previously described[16] was delivered into a monolayer of smooth muscle cells via the WPI Pneumatic PicoPump (PV 820) on a Leica MZ16. Glass capillaries (TW100F-40) were pulled to inject Lucifer Yellow (~1.2 nL). Post-injection, confocal fluorescence images were acquired using the Nikon SoRa spinning disk microscope, as described earlier, with the 20×LambdaS apochromat (N.A. 0.95) water immersion lens, and Tokai Hit Stage Top Incubator to control temperature, humidity, and CO_2.

Extended field of view confocal images were collected covering a total area of 9.21 mm^2. The tiled images were stitched together into a single large image using the Nikon Elements software (v. 5.3). The stitched images were background subtracted, and the mean fluorescence intensity of Lucifer Yellow positive cells was measured for both mutant and WT cells using the Cellpose 2.0 AI-based image segmentation algorithm with built-in cyto2 model,[17] run through Arivis Vision 4D (v. 3.6) image analysis software (Arivis Imaging, Inc., Boston, MA).

Results

Thra1$^{PV/+}$ *mice exhibit colonic abnormalities mimicking constipation in patients with mutations of TRα1*

Figure 1A shows that the body weight of *Thra1*$^{PV/+}$ mice was decreased by 43% as compared with WT mice.[13] Evaluation of colonic motility showed that the average colonic transit time for WT mice was 2.58±0.95 minutes (n=22), and for the *Thra1*$^{PV/+}$ mice was 7.97±5.61 minutes (n=26) (Fig. 1B). The colonic transit time was 3.09-fold longer in *Thra1*$^{PV/+}$ mice than in WT mice. Interestingly, the water content was 42% lower in *Thra1*$^{PV/+}$ mice than in WT mice (Fig. 1C) and the length of the colon was longer (Fig. 1D-a, with content; D-II-b, content flushed). These observations indicate that *Thra1*$^{PV/+}$ mice manifest the constipation phenotype.

The rectum of Thra1$^{PV/+}$ *mice manifests histopathological defects*

Analysis of rectum tissues stained by Periodic acid Schiff (PAS) revealed distinct histological differences between WT and *Thra1*$^{PV/+}$ mice. In the WT mice, the colonic crypts were tightly and orderly aligned (Fig. 2A-a). In contrast, in *Thra1*$^{PV/+}$ mice, colonic crypts were loosely aligned with enlarged interstitium space around the crypt bases, particularly prominent in the lamina propria (Fig. 2A-b). It is of interest to note that the area of muscularis mucosae was expanded by ~40% (Fig. 2A-II-b). The submucosa is a fibrous connective tissue layer that surrounds the mucosa and is composed of collagen fibers[18] that can be stained with Masson's Trichrome.

As shown in Figure 2B-I, collagen staining (shown in blue) showed that the submucosa of the rectum in *Thra1*$^{PV/+}$ mice (panel b) was more expanded as compared with WT mice (panel b). Measurement of area showed that the submucosae was 1.5-fold larger in *Thra1*$^{PV/+}$ mice than in WT mice (Fig. 2B-II). Analysis of the collagen content in the rectum showed that the collagen levels were increased three-fold (Fig. 2B-III-a, -b), supporting that the connective tissues

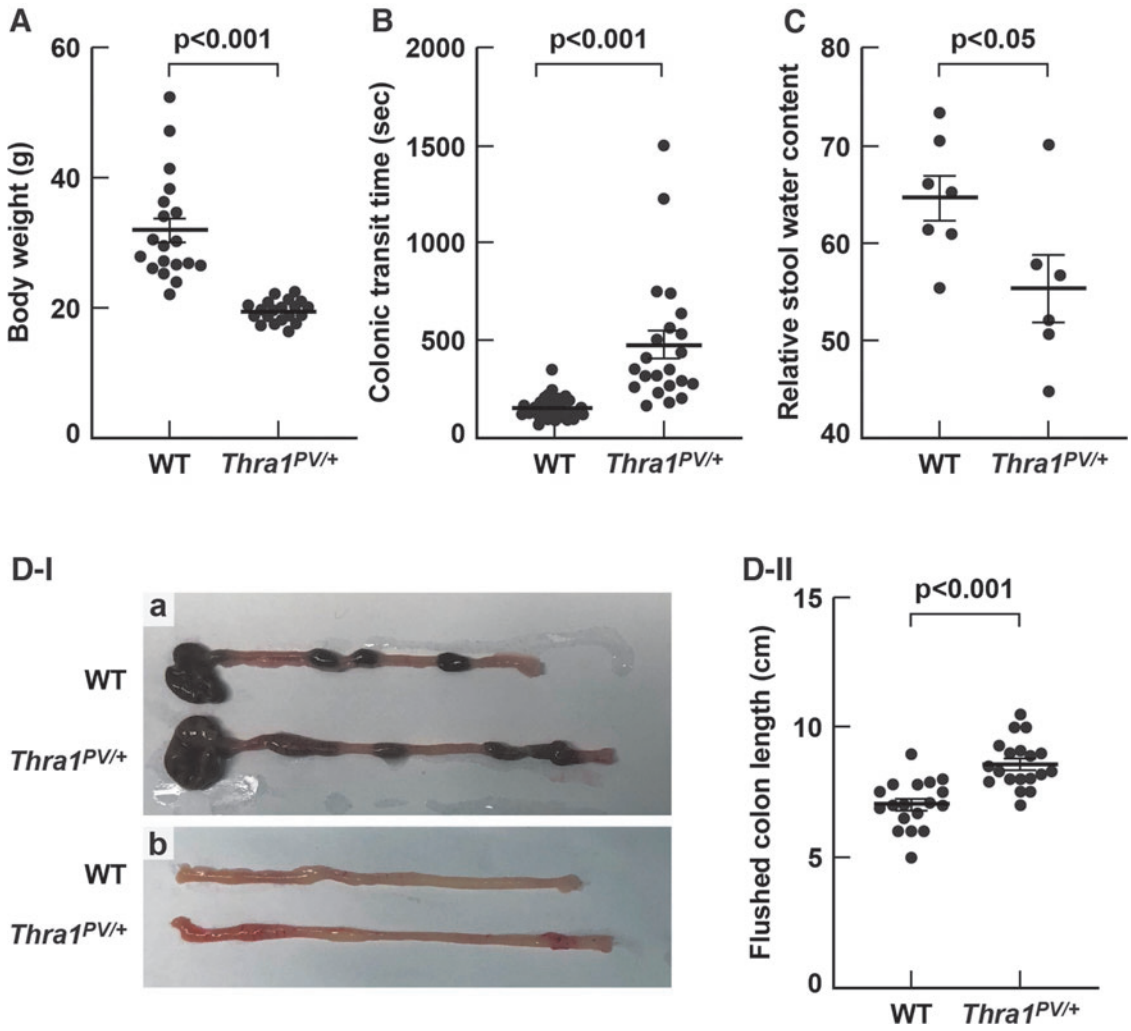

FIG. 1. Colonic defects in *Thra1*$^{PV/+}$ mice. (**A**) Decreased body weight in female *Thra1*$^{PV/+}$ mice ($n=21$) as compared with female WT mice ($n=19$), mouse age: 3.9–8.4 months. (**B**) Increased colonic transit time in *Thra1*$^{PV/+}$ mice ($n=22$) as compared with WT mice ($n=26$), mouse age: 3.9–7.4 months. (**C**) Decreased water content in the stool of *Thra1*$^{PV/+}$ mice ($n=6$) as compared with WT mice ($n=7$), mouse age: 2.6–7.4 months. (**D-I-a**) Representative example of longer colon length with the content. **(D-I-b)** Representative example of longer colon length without the content, after the content was flushed out. (**D-II**) Quantitative data to show longer colon length in *Thra1*$^{PV/+}$ mice ($n=19$) as compared with WT mice ($n=18$) after the content was flushed out. Values are means ± SEM. The *p*-values are indicated. WT, wild type.

were abnormally expanded, which could derail the transport of fluid and electrolytes in and out of adjacent smooth muscle cells of *Thra1*$^{PV/+}$ mice.

One structural element in the smooth muscle that is critical in the intercellular communication is the gap junction. Gap junctions are channels that directly connect the cytoplasm of adjacent cells, allowing the flow of small molecules, ions, and electrical signals to pass through a regulated gate between cells.[19] Gap junctions can be unequivocally identified by TEM. Figure 3 shows the representative TEM images of rectum smooth muscle cells of WT mice and *Thra1*$^{PV/+}$ mice at the age of 2.6 months (panels a–d) and 7.2 months (panels e–h).

No apparent abnormalities were discernable for nucleus, mitochondria, Golgi apparatus, and ribosomes in the muscle cells of *Thra1*$^{PV/+}$ mice. However, at the age of 2.6 months, compared with WT mice, *Thra1*$^{PV/+}$ mice exhibited abnormal fibers, frequently twisted (marked by an asterisk* in Fig. 3, at lower magnification of 2 μm, panel b vs. panel a), with wider gaps between muscle cells (red arrows; panel b). As shown in Figure 3, at higher magnification of 500 nm, abundant caveolae (marked by solid arrowhead, panel c) and vesicles (marked by blue arrowheads) were visible in WT mice. In contrast, at the same magnification, fewer caveolae and vesicles were observed in *Thra1*$^{PV/+}$ mice (panel d).

Similar shorter fibers with wider gaps (Fig. 3, panel f vs. panel e) and reduced numbers of caveolae, and vesicles were found in the smooth muscle of *Thra1*$^{PV/+}$ mice at the older age of 7.2 months (Fig. 3, panel h vs. g). These results indicate that the defects occur at the early age of 2.6 months, persisting into older age.

Gap junction functions are impaired in the rectum smooth muscle of Thra1$^{PV/+}$ *mice*

The abnormal structure of gap junctions and other membrane-associated sub-cellular organelles revealed by

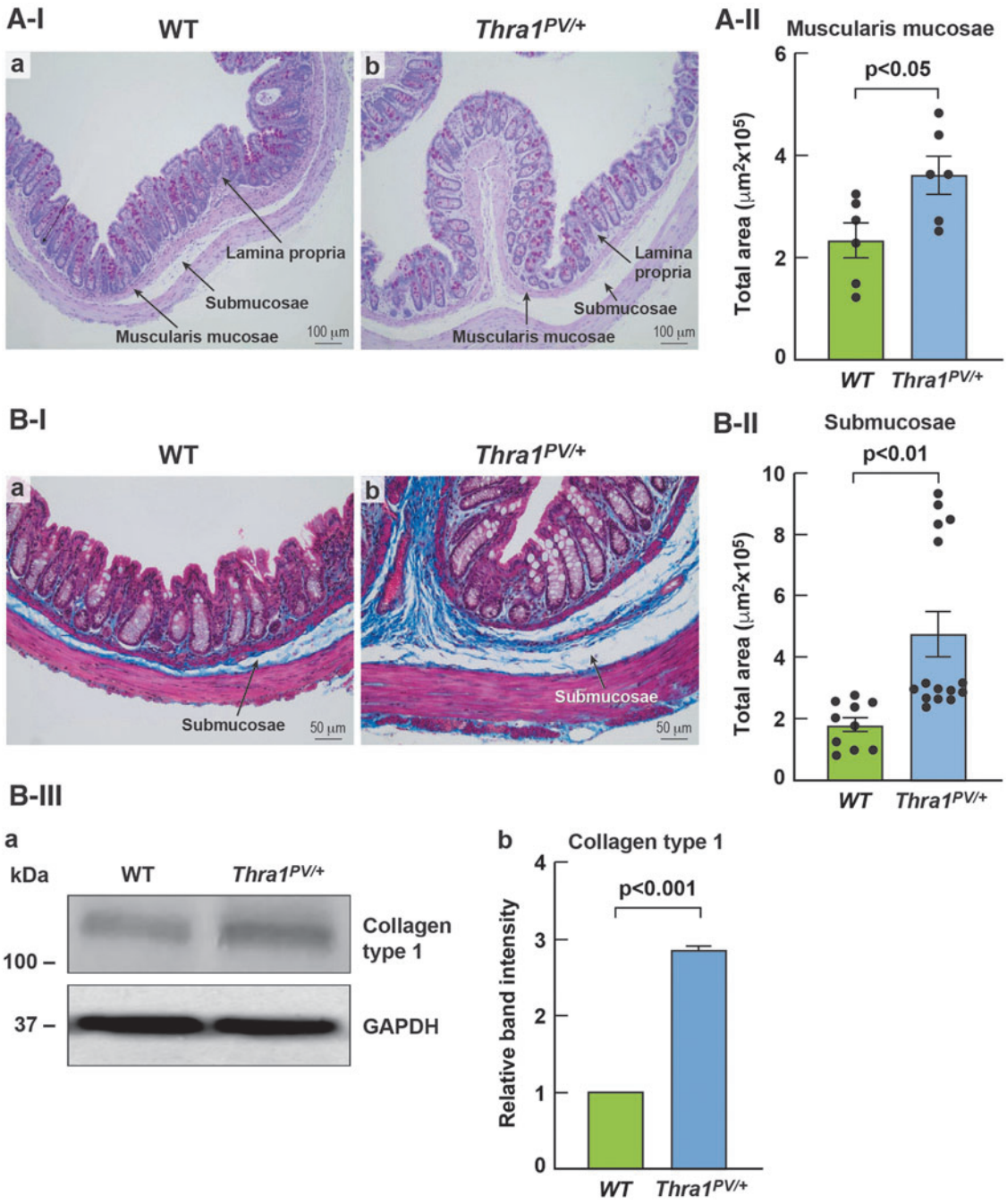

FIG. 2. Histopathological abnormalities in the rectum of *Thra1*$^{PV/+}$ mice. (**A-I**) PAS staining of rectum of WT mice (panel a; $n=6$) and *Thra1*$^{PV/+}$ mice (panel b; $n=6$), mouse age: 6.1–7.5 months. Scale bar = 100 μm; the sub-structural elements are marked. (**A-II**) Comparison of total areas of muscularis mucosae of WT ($n=6$) and *Thra1*$^{PV/+}$ mice ($n=6$). (**B-I**) Masson's Trichrome staining of rectum of WT mice (panel a; $n=6$) and *Thra1*$^{PV/+}$ mice (panel b; $n=6$). (**B-II**) Comparison of total areas of submucosae of WT ($n=6$) and *Thra1*$^{PV/+}$ mice ($n=6$). (**B-III-a**) Representative Western blot of collagen type 1 in the rectum of WT ($n=3$) and *Thra1*$^{PV/+}$ mice ($n=3$). (**B-III-b**) Increased collagen type 1 in the rectum of *Thra1*$^{PV/+}$ mice ($n=3$) as compared with WT mice ($n=3$). Values are means ± SEM. The *p*-values are indicated. PAS, Periodic acid Schiff.

TEM prompted us to investigate the functional consequences of these changes in *Thra1*$^{PV/+}$ mice. To do so, we isolated smooth muscle cells from rectums of WT and *Thra1*$^{PV/+}$ mice to assess the ability of intercellular transfer of small molecules. Using confocal imaging, we showed that the smooth muscle cells isolated from rectum of WT and *Thra1*$^{PV/+}$ mice exhibited characteristic smooth muscle actin fibers evidenced by immuno-stained actin fibers using anti-α-smooth muscle actin antibodies, establishing the identity of smooth muscle cells (Supplementary Fig. S1A-a, -b).

We further demonstrated no changes in the protein levels of α-smooth muscle actin in the smooth muscle cells isolated from WT and *Thra1*$^{PV/+}$ mice (Supplementary Fig. S1B-a, -b). We demonstrated the existence of gap junctions in the

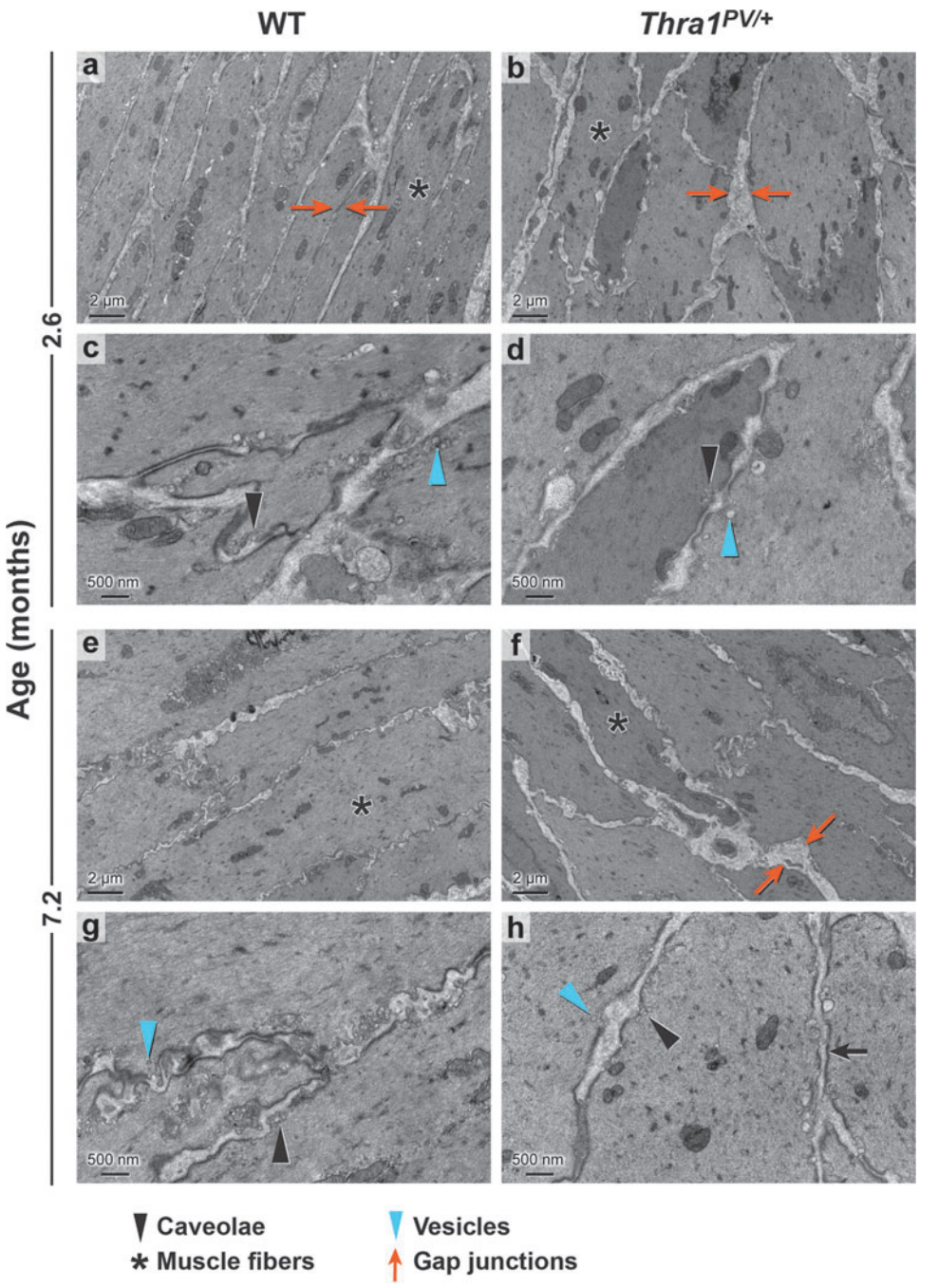

FIG. 3. Transmission electron microscopy revealed defects in the smooth muscles of *Thra1*$^{PV/+}$ mice. Representative micrographs of WT ($n=4$) and *Thra1*$^{PV/+}$ mice ($n=4$) at the age of 2.6 months (panels **a–d**) and 7.2 months (panels **e–h**). The scale is 2 μm in panels (**a, b,** and **e**) and 500 nm in panels (**c, d, g,** and **h**). Individual muscle fibers are smaller in the mutant mice with wider gaps between fibers. The vesicles and caveolae are reduced in the *Thra1*$^{PV/+}$ mice. The symbol representations of sub-cellular organelles are marked as shown.

isolated rectum smooth muscle cells by a gap junction marker, connexin 43 using super-resolution imaging. Figure 4A-a shows the confocal green fluorescence image for the localization of connexin 43 on the cell membrane of rectal small muscle cells isolated from WT mice.

The cell boundaries were marked by the MemBrite plasma membrane stained red. Panel b shows the overlay of green fluorescence signals with MemBrite red signals to indicate that connexin 43 was localized on the membrane junctions of the neighboring cells (marked by a white box). We also detected the localization of connexin 43 on the cell membrane of rectum smooth muscle cells of *Thra1*$^{PV/+}$ mice (Fig. 4A-c, green fluorescence signals), which were more clearly visualized in the overlaying of green fluorescence signals with the cell membrane marker, red MemBrite (marked by a box in panel d). These findings indicate that the smooth muscle cells isolated from rectums of WT and *Thra1*$^{PV/+}$ mice could form gap junctions *in vitro*.

We next assessed whether the gap junction defects revealed by TEM could affect the intercellular communication by using a fluorescence tracer, Lucifer Yellow.[20,21] Lucifer Yellow has been extensively used to study cell structure and intercellular communication.[22,23] We microinjected identical amounts of Lucifer Yellow into similar numbers of smooth muscle cells isolated from WT and *Thra1*$^{PV/+}$ mice. We captured the fluorescence images at an identical time

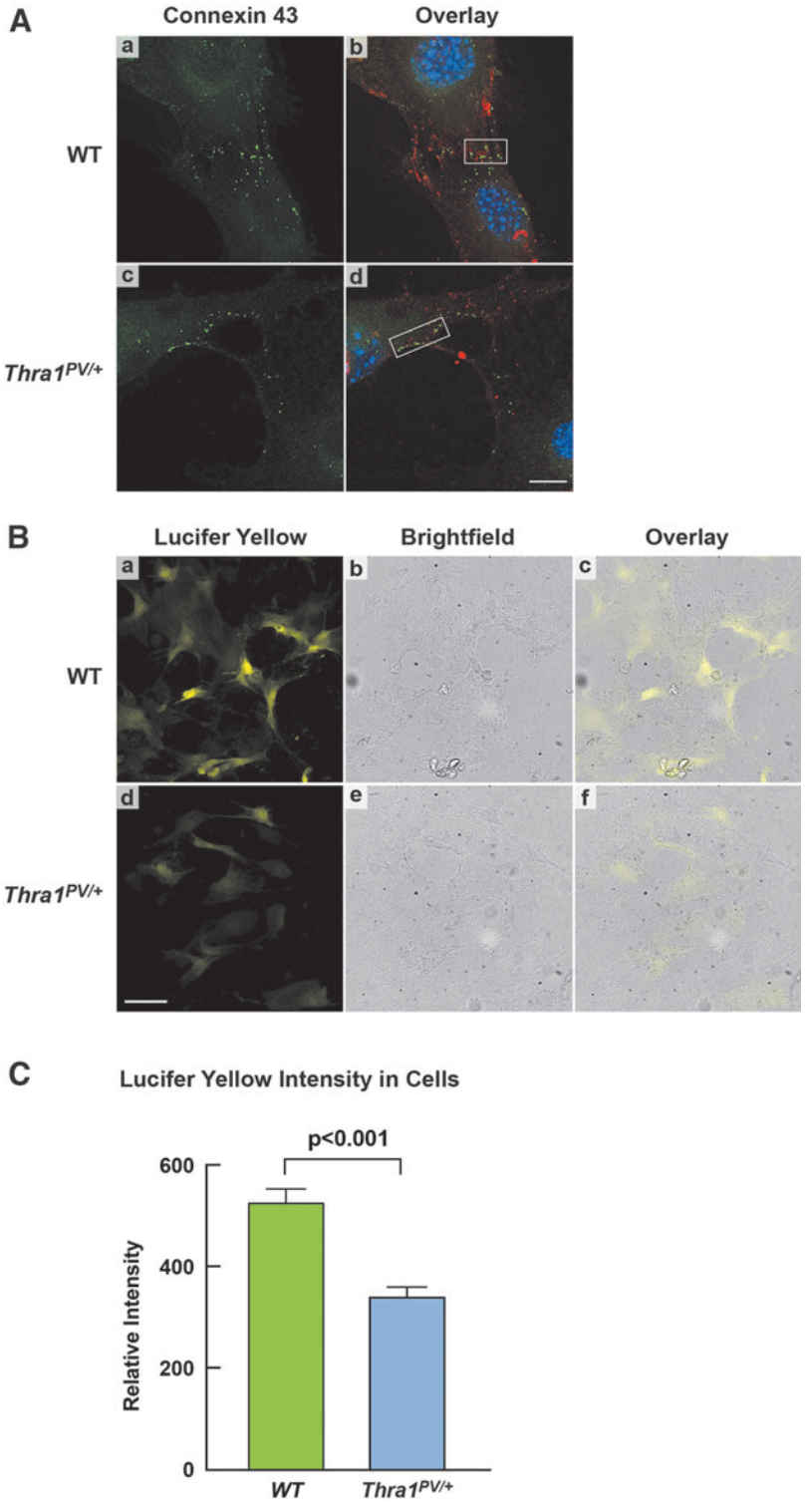

FIG. 4. Confocal images of gap junctions and defective intercellular transfer of Lucifer Yellow in the isolated rectal smooth muscle cells of *Thra1*$^{PV/+}$ mice. (**A**) Maximum intensity projections of super-resolution z-stacks are shown with Connexin 43 in green (panel **a**), and the overlay of Connexin 43, MemBrite, and 4′,6-diamidino-2-phenylindole in the right column (panel **b**). The gap junction shown by Connexin 43 marker on the membrane is marked by the boxes. WT cells are shown in the top row (panels **a, b**), and cells isolated from *Thra1*$^{PV/+}$ mice are in the bottom row (panels **c** and **d**). Scale bar equals 10 μm for all image panels. (**B**) Single confocal (panels **a, d**) and brightfield images of cells microinjected with Lucifer Yellow (panels **b, e**) and the overlay of fluorescence images with bright field images (panel **c, f**). WT cells are shown in the top row (panels **a–c**), and cells isolated from *Thra1*$^{PV/+}$ mice are in the bottom row (panels **d–f**). Cells were isolated from mice at the age: $\sim$7.4 months. Scale bar equals 100 μm in all image panels. (**C**) The Lucifer Yellow intensity in smooth muscle cells isolated from *Thra1*$^{PV/+}$ mice was reduced. Similar number of cells per area were microinjected. We measured both the mean intensity of Lucifer Yellow fluorescence per cell in an extended field of view area $\sim$9 mm^2. Cells with Lucifer Yellow fluorescence intensity above the background were considered positive. We observed more lucifer yellow positive cells per area in the WT sample compared with the mutant cells. The fluorescence intensity was determined in 227 and 230 cells in images of WT no.1 and WT no.2, respectively, and was 196 and 220 cells for mutant no.1 and mutant no.2, respectively.

(10 minutes) post micro-injection to allow sufficient time for the tracer dye to transfer into neighboring cells.

As shown in Figure 4B, fewer yellow fluorescent smooth muscle cells were detected in *Thra1*$^{PV/+}$ mice than WT mice (panel d vs. panel a). Moreover, the fluorescence intensity in the cells from *Thra1*$^{PV/+}$ mice was clearly weaker than that in the WT mice (panels d vs. a). Figure 4B-b and -e show the corresponding bright field to demonstrate that similar number of cells were present in the field imaged by confocal fluorescence microscopy. Panels c and f show the overlay of fluorescence images with the bright field imaging, demonstrating that Lucifer Yellow fluorescence is in the cells that are in contact with the neighboring cells.

To provide quantitative assessment, we measured both the mean intensity of Lucifer Yellow fluorescence per cell and the number of Lucifer Yellow positive cells in an extended

field of view area $\sim 9\,mm^2$. Cells with Lucifer Yellow fluorescence intensity above the background were considered positive. The quantitative data indicated that the mean intensity of Lucifer Yellow fluorescence in the mutant cells was 35% lower than in the WT cells (Fig. 4C). Taken together, these findings indicate that the intercellular communication in the smooth muscles of *Thra1*$^{PV/+}$ mice is impaired due to defective gap junctions.

Suppression of smooth muscle contractile regulators in the rectum of Thra1$^{PV/+}$ *mice*

The abnormality in the gap junctions and the expanded muscularis mucosa and submucosa suggested that the contractility of smooth muscle in the rectum could be impaired. Figure 5A shows the major regulatory circuit in the control of smooth muscle contractility. Binding of Ca^{+2} to calmodulin results in conformational change in the calmodulin to interact with myosin light-chain kinase (MLCK), leading to the phosphorylation of myosin light chain (MLC), allowing myosin II to interact with actin to initiate contraction of smooth muscles. The myosin light chain phosphatases (MLCP) acts to dephosphorylate MLC to relax the contractility. Rho kinase (ROCKs) serve as inhibitors to suppress the activity of MLCP for additional regulation of the regulatory circuit.[24,25]

Analysis of the protein levels showed that calmodulin abundance was lower in the rectum of *Thra1*$^{PV/+}$ mice (Fig. 5B-I-a and B-II-a). Consistent with lower protein abundance of MLCK (Fig. 5B-I-c and B-II-b), the ratios of p-MLC/total MLC were markedly lower (Fig. 5B-I-d and e, and B-II-c), without changing the protein levels of myosin heavy chain (MYH 11; B-I-g) and α-SMA actin (B-I-i and B-II-e). The protein levels of myosin light chain phosphatase (MYPT1) were lower (B-I-l and B-II-f).

The decreased protein levels of ROCK1 (Rho kinase; B-I-l and B-II-g) were lower, and they allowed MYPT1 to dephosphorylate MLC to further hinder the contractility of the rectum in *Thra1*$^{PV/+}$ mice. Taken together, these changes reduced the contractility of smooth muscle cells, which could lead to slow transit time and constipation. Similar regulatory patterns in the isolated smooth muscle cells were observed as in the rectum tissues (Supplementary Fig. S2), indicating that isolated smooth muscle cells retained similar functional characteristics as in the rectum tissues, and they therefore can be used for functional analysis.

Impaired ICC in the rectum of Thra1$^{PV/+}$ *mice*

To further explore other mechanisms that could contribute to the constipation observed in patients with mutation of the *THRA* gene, we evaluated potential defects in rectum ICC of *Thra1*$^{PV/+}$ mice. Extensive studies have shown that ICC function as pacemakers to provide a means to coordinate proper propagation of contractions and motility movement. The ultrastructure by TEM (2500× magnification) shows that ICC in the rectal smooth muscles of *Thra1*$^{PV/+}$ mice exhibited marked reduced (hypoplastic) cytoplasm (Fig. 6; panel b, marked by blue arrowheads) as compared with WT smooth muscles (panel a).

All clearly identifiable organelles such as mitochondria appeared normal in size, shape, and structures; however, the cytoplasm appeared to be more condensed in ICC of *Thra1*$^{PV/+}$ mice (panels b vs. a, marked by blue arrowheads). The more compacted disorganized mitochondria in ICC of *Thra1*$^{PV/+}$ mice could be viewed more clearly at a higher magnification (3000×) shown in Figure 6d (marked by yellow arrowheads). The hypoplastic ICC in the rectum smooth muscles of *Thra1*$^{PV/+}$ mice suggested the impaired maturation of ICC.

We next ascertained whether the numbers of ICC could be affected in the rectum smooth muscles cells of *Thra1*$^{PV/+}$ mice. The c-KIT receptor tyrosine kinase (c-KIT) is known to regulate the development of ICC[26] and has been used as a marker for ICC in the smooth muscle cells.[27] Identification of ICCs was based on c-KIT immunohistochemical staining, localization, and morphologic characteristics of cells by a board-certified veterinary pathologist. The number of c-KIT positive cells was quantified per millimeter within the submucosal region (black arrows, Fig. 7A-I) and in the myenteric plexus (blue arrows, Fig. 7A-I).

Quantitative analysis shows a 70% and 45% reduction of ICC in the submucosa and rectum myentyeric plexus, respectively (Fig. 7A-II, upper panel and lower panel, respectively). The hypoplasia with a reduction in numbers of ICC could lead to weakened motility and slow colonic transit in *Thra1*$^{PV/+}$ mice.

The hypoplastic ICC prompted us to ascertain whether the c-KIT signaling is affected in rectum of *Thra1*$^{PV/+}$ mice. The c-KIT, a receptor tyrosine kinase and its cognate ligand SCF (stem cell factor), are abundantly expressed in the smooth muscle cells of gastrointestinal tract.[28] The interaction of SCF with c-KIT results in downstream signal transduction to affect proliferation, differentiation, and function of ICC.[27,28] Indeed, we found that protein levels of c-KIT (Fig. 7B-I-a and quantitative data in Fig. 7B-II-a) and SCF (Fig. 7B-I-c and quantitative data in Fig. 7B-II-b) were reduced.

One of the downstream effectors of c-KIT signaling is c-Src, a non-receptor-type tyrosine kinase, which is critical in cell growth, differentiation, migration, and survival. We found that the ratios of p-c-Src (Fig. 7B-I, panel e) as well as the ratios of p-c-Src/total c-Src (Fig, 7B-II-c) were reduced. The findings indicate that TRα1 mutants suppressed the expression of c-KIT and its ligand to attenuate c-KIT signaling via c-Src as one of the downstream pathways to impede the development of ICC.

FIG. 5. Suppression of smooth muscle contractile regulators in the rectum of *Thra1*$^{PV/+}$ mice. (**A**) Schematic representation of regulatory circuit in the contractility of rectal smooth muscles. All regulators are marked. (**B-I**) Analysis of the protein levels of key regulators of contractility in rectum of WT ($n=3$) and *Thra1*$^{PV/+}$ mice (age: 3.9–8.5 months). Representative Western blot of key contractile regulators and their respective loading controls are shown. Each Western blot analysis was from the rectum of WT ($n=3$) and *Thra1*$^{PV/+}$ mice ($n=3$). (**B-II**) Quantitative analysis of the band intensities in blots shown (**B-I**) for each regulator ($n=3$). Values are means ± SEM. The *p*-values are indicated.

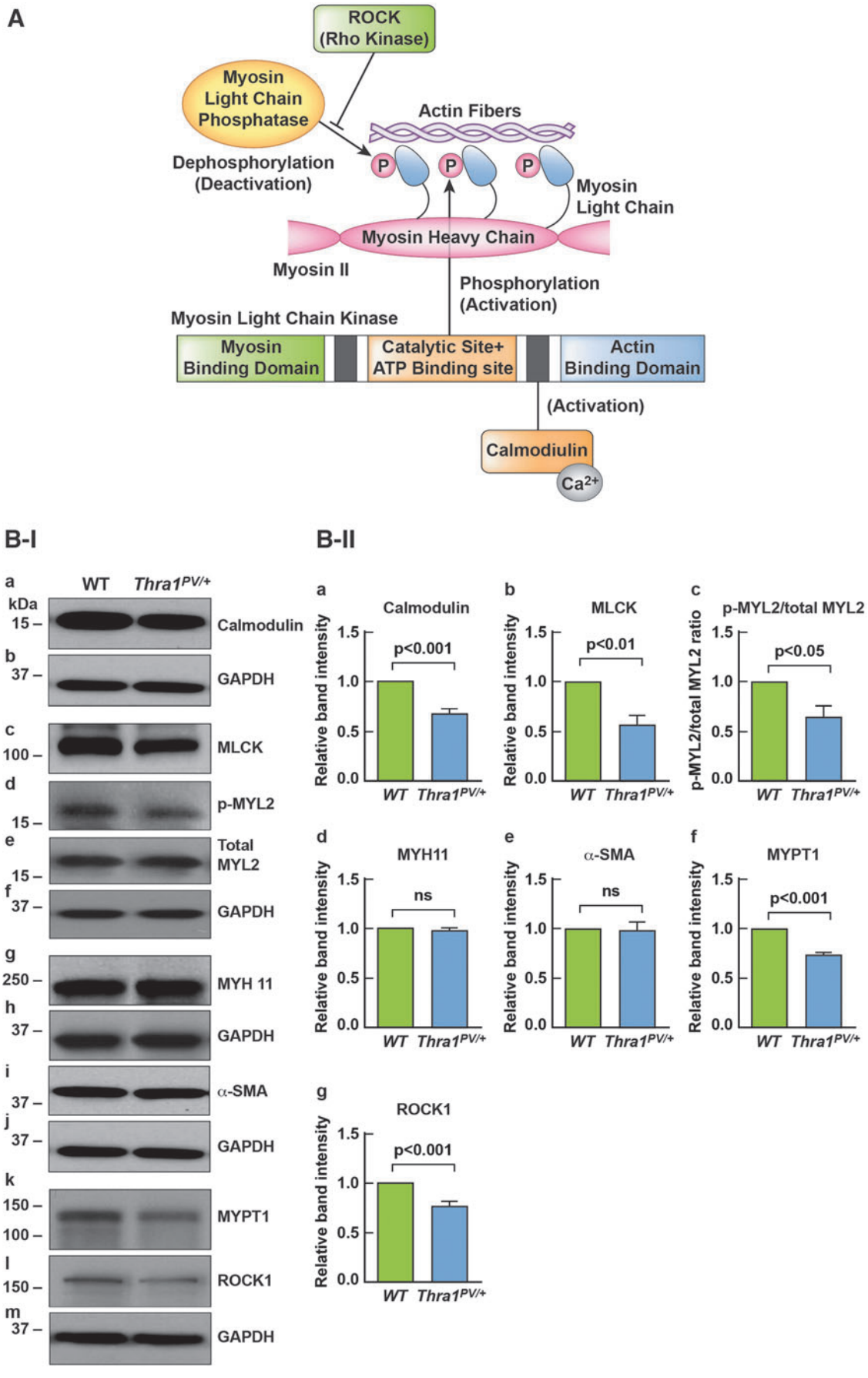
A
ROCK
(Rho Kinase)
Myosin
Light Chain
Phosphatase
Actin Fibers
Dephosphorylation
(Deactivation)
P
P
P
Myosin
Light Chain
Myosin Heavy Chain
Myosin II
Phosphorylation
(Activation)
Myosin Light Chain Kinase
Myosin
Binding Domain
Catalytic Site+
ATP Binding site
Actin
Binding Domain
(Activation)
Calmodiulin
Ca2+
B-I
a
WT
Thra1PV/+
kDa
15 –
Calmodulin
b
37 –
GAPDH
c
100 –
MLCK
d
p-MYL2
15 –
e
Total
MYL2
15 –
f
37 –
GAPDH
g
250 –
MYH 11
h
37 –
GAPDH
i
37 –
α-SMA
j
37 –
GAPDH
k
150 –
100 –
MYPT1
l
150 –
ROCK1
m
37 –
GAPDH
B-II
a
Calmodulin
Relative band intensity
p<0.001
b
MLCK
p<0.01
c
p-MYL2/total MYL2
p-MYL2/total MYL2 ratio
p<0.05
d
MYH11
ns
e
α-SMA
ns
f
MYPT1
p<0.001
g
ROCK1
p<0.001
1.5
1.0
0.5
0.0
WT
Thra1PV/+

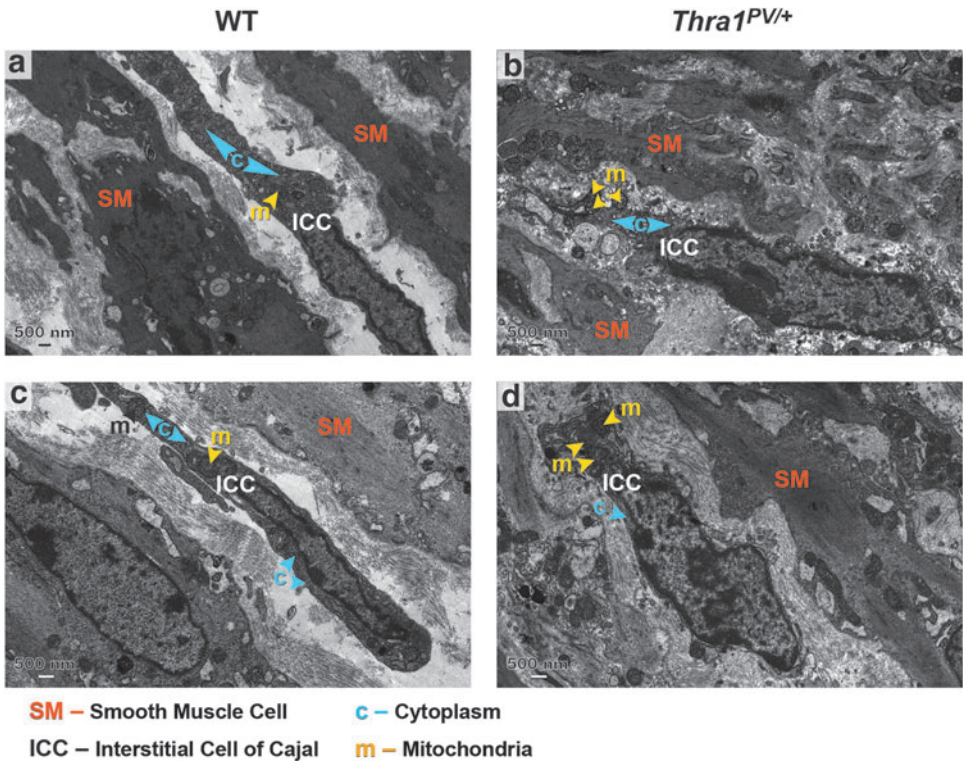

FIG. 6. Transmission electron microscopy detects hypoplastic ICC in the rectum smooth muscle cells of *Thra1*$^{PV/+}$ mice. Representative micrographs of WT ($n=4$) and *Thra1*$^{PV/+}$ mice ($n=4$) at 7.2 months. The magnification of images in panels are marked. The ICC in the rectal smooth muscle cells of *Thra1*$^{PV/+}$ mice have significantly reduced (hypoplastic) cytoplasm (panels **b, d**) as compared with the WT muscle cells (panels **a, c**). All clearly identifiable organelles appeared to be more condensed in the *Thra1*$^{PV/+}$ mice. The symbol representations of sub-cellular organelles are marked. ICC, interstitial cells of Cajal.

Discussion

The discovery of patients with mutations of the *THRA* gene has marked a milestone in understanding the *in vivo* actions of TRα1 mutants. Significant progress has been made in elucidating how TRα1 mutants cause pathological manifestations of RTHα in the bone and erythropoiesis by using the *Thra1*$^{PV/+}$ mouse, a model RTHα.[7–11] In the present studies, we provided evidence to show how mutations of TRα1 impacted the morphology and the colonic functions. The colonic transit time was markedly prolonged and accompanied by decreased water content in the feces in *Thra1*$^{PV/+}$ mice.

We found enlarged space between the columns of crypts, especially at the junctions with muscularis mucosae. The connective tissue in the submucosa appeared to be loose and expanded with an increased amount of collagen (Fig. 2B-III a and b). The TEM revealed enlarged space in the gap junctions of smooth muscle cells with decreased numbers of caveolae and vesicles, which could adversely affect effective transport of intercellular fluid, small signaling molecules, and electrolytes. Indeed, functional assays by confocal imaging of the intercellular movement of a fluorescence dye (Lucifer Yellow) clearly showed that the intercellular transfer activity of smooth muscle cells was impaired in the rectum muscle cells of *Thra1*$^{PV/+}$ mice.

We further discovered that ICC were hypoplasia with reduction in numbers in the rectum smooth muscles of *Thra1*$^{PV/+}$ mice and that the expression of key contractile regulators was significantly decreased. Collectively, these morphological defects in the gap junctions, submucosae, muscularis mucosae and ICC, contribute to weakening the colonic activity. These findings have provided new insights into the molecular basis underlying the impeded colonic activity, leading to constipation in patients with mutations of the *THRA* gene.

The identification of abnormalities in ICC (hypoplastic as well as reduced number) in the rectum smooth muscle cells of *Thra1*$^{PV/+}$ mice shed new light on the understanding of the weakened colonic motility in RTHα patients. The ICC, electrically coupled to smooth muscle cells, is responsible to initiate intrinsic pacemaker activity.[25] Gastrointestinal smooth muscle tissues such as the colon possess spontaneous intrinsic pacemaker activity that organizes into phasic contractions, which is the basis for peristaltic activity.

The defective ICC found in the rectum of *Thra1*$^{PV/+}$ mice would be less effective to initiate the rhythmicity and contractions of rectum. Together with the wider gap junctions between the smooth muscle cells and the decreased abundance of key smooth muscle contractile regulators, the coordinated movement is further impeded in the rectum of *Thra1*$^{PV/+}$ mice. However, although the intrinsic neural plexuses allow a significant degree of autonomy in the gastrointestinal tract functions, it is also known that extrinsic neural inputs from the central nervous system could modulate to further fine tune its activity.

At present, it is unknown how mutations of the *THRA* gene could impact the basic neural circuitry of the parasympathetic and sympathetic neural inputs to the gastrointestinal tract. The elucidation of the actions of mutant TRα1 on the neural circuitry would await future studies.

It has long been known that constipation or obstipation frequently occurs in hypothyroid patients.[29] However, very few studies have examined how hypothyroidism could cause the constipation in patients. Subsequently, with the creation of mutant mice deficient in the *Thrb* gene (*Thrb*$^{-/-}$ mice), the *Thra* gene (*Thra*$^{-/-}$ mice), or both the *Thrb* and *Thra* genes

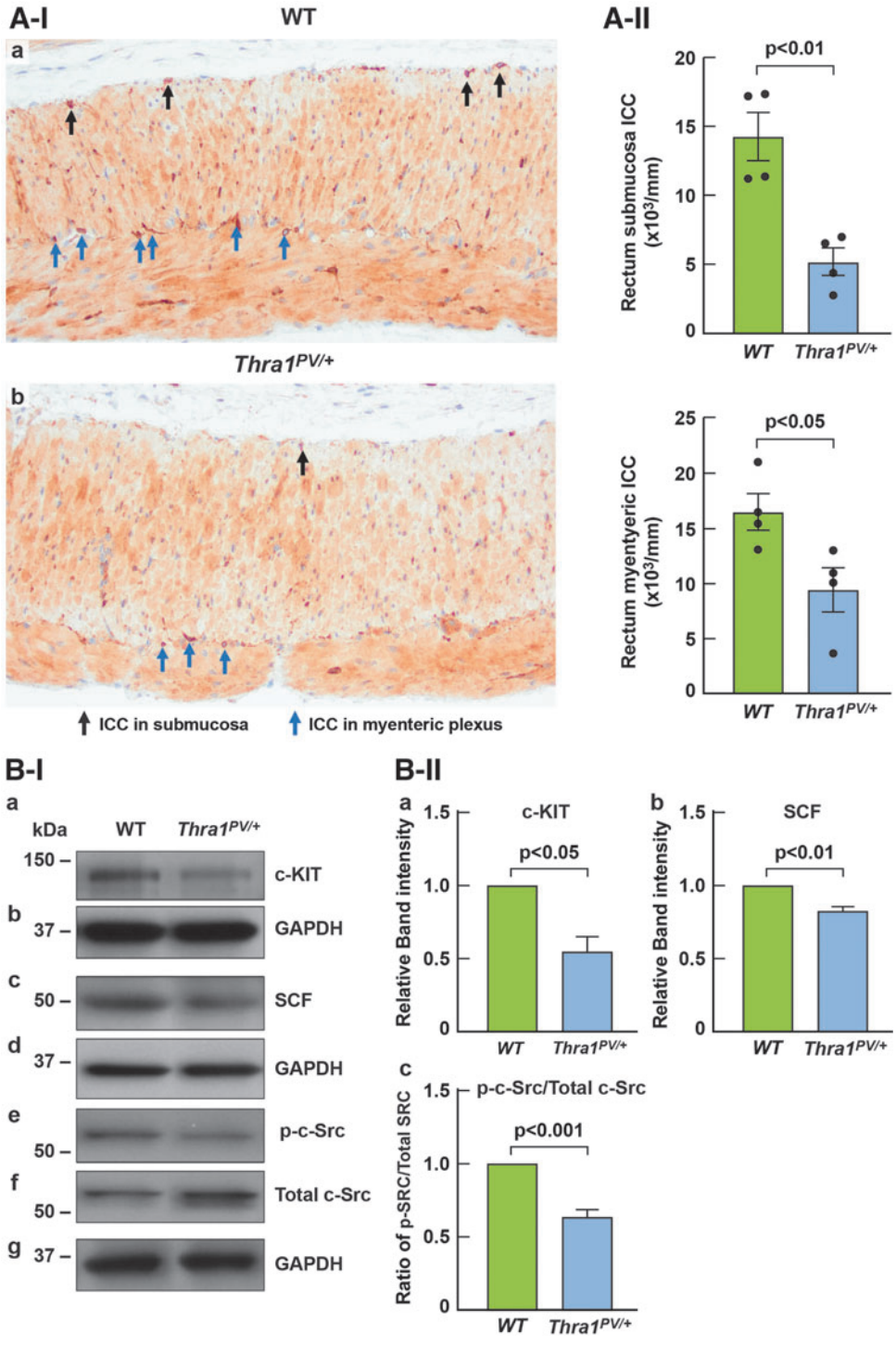

FIG. 7. Reduced ICC in the rectum submucosa and myenteric plexus of *Thra1*$^{PV/+}$ mice. (**A-I**) Representative micrographs of WT (panel **a**; $n=4$) and *Thra1*$^{PV/+}$ mice (panel **b**: $n=4$) at 5–6 months. ICC was identified by immunohistochemical analysis using anti-c-KIT antibodies. (**A-II**) Quantitative analysis of c-KIT positive ICC in submucosae (upper panel) and in myenteric plexus (lower panel). Values are means ± SEM. The *p*-values are indicated. (**B**) Analysis of the protein levels of C-KIT, SCF, and c-SRC in rectum of WT ($n=3$) and *Thra1*$^{PV/+}$ mice. Representative Western blots of these regulators are as shown, and their respective loading controls are shown (**B-I**). Quantitation of the band intensities are shown in **(B-II**). Values are means ± SEM ($n=3$). The *p*-values are indicated. SCF, stem cell factor.

(*Thrb*$^{-/-}$*Thra*$^{-/-}$ mice), it is possible to assess the role of each TR isoform in the biology of the intestine and colon.

Studies indicated that *Thrα*$^{-/-}$ mice showed reduced length of the intestine with a greater fragility compared with WT mice. This was also observed in the *Thrb*$^{-/-}$*Thra*$^{-/-}$ mice. On the contrary, no differences between WT and *Thrb*$^{-/-}$ mice were found,[30,31] indicating the critical role of TRα1 in the development and functions of the intestine. Histological analysis of the proximal and distal parts of the small intestine showed decreased intestinal size and the length of the crypt-villus unit in the *Thrα*$^{-/-}$ mice compared with WT mice, but no apparent abnormalities were detected in the colons of *Thrα*$^{-/-}$ mice.

These observations are in contrast with the longer intestine and colon observed in mice expressing dominant negative TRα1 mutant (*Thra1*$^{PV/+}$ mice[12]; and the present studies). Moreover, in the present studies, extensive morphological defects in the lamina propria, muscularis mucosae, submucosae, gap junctions, and ICC, as well as functional colonic deficiencies were detected in *Thra1*$^{PV/+}$ mice. These

findings indicate that the loss of normal TRα1 function, due to gene knockout and expression of a dominant negative TRα1 mutant, clearly led to distinct functional consequences in the pathology of the intestine and the colon.

The constipation due to hypothyroidism is mediated by insufficient thyroid hormone levels, but with normal functional TRs. The constipation in RTHα is due to the resistance to thyroid hormone in the presence of normal thyroid hormones because of mutated TRα1. These distinct molecular actions *in vivo* would suggest that the treatment for constipation due to hypothyroidism or RTHα would require the consideration of different therapeutic approaches.

Acknowledgments

The authors thank Christopher King for assistance in the preparation of TEM micrographs. They are grateful to Ross Lake for scanning PAS-stained rectum slides for measurement of areas of muscularis mucosae and submucosae. They thank Mark Willingham for assistance in the insightful interpretation of the histological analysis. They also thank Joelle Mornini, NIH Library, for article editing assistance.

Authors' Contributions

Conception and designs were performed by S.-Y.C. and M.K.; development of methodology and acquisition of data were carried out by M.K., V.H., P.Z., K.B., E.E., W.K.L.D., and S.-Y.C. Analysis and interpretation of data were performed by M.K., S.-Y.C., V.H., P.Z., K.B., E.E., and Y.-J.Z.; writing, review, and/or revision were performed by S.-Y.C. and M.K. Administrative, technical, or material support was organized by S.-Y.C.

Author Disclosure Statement

No competing financial interests exist.

Funding Information

This research is supported by the Intramural Research Program of the Center for Cancer Research, National Cancer Institute, National Institutes of Health (ZIA BC 008752).

Supplementary Material

Supplementary Data
Supplementary Figure S1
Supplementary Figure S2

References

1. Bochukova E, Schoenmakers N, Agostini M, et al. A mutation in the thyroid hormone receptor alpha gene. N Engl J Med 2012;366(3):243–249; doi: 10.1056/NEJMoa1110296
2. van Mullem A, van Heerebeek R, Chrysis D, et al. Clinical phenotype and mutant TRα1. N Engl J Med 2012;366(15): 1451–1453; doi: 10.1056/NEJMc1113940
3. Demir K, van Gucht AL, Büyükinan M, et al. Diverse genotypes and phenotypes of three novel thyroid hormone receptor-α mutations. J Clin Endocrinol Metab 2016; 101(8):2945–2954; doi: 10.1210/jc.2016-1404
4. Tylki-Szymańska A, Acuna-Hidalgo R, Krajewska-Walasek M, et al. Thyroid hormone resistance syndrome due to mutations in the thyroid hormone receptor α gene (THRA). J Med Genet 2015;52(5):312–316; doi: 10.1136/jmedgenet-2014-102936
5. Moran C, Chatterjee K. Resistance to thyroid hormone due to defective thyroid receptor alpha. Best Pract Res Clin Endocrinol Metab 2015;29(4):647–657; doi: 10.1016/j.beem.2015.07.007
6. van Mullem AA, Chrysis D, Eythimiadou A, et al. Clinical phenotype of a new type of thyroid hormone resistance caused by a mutation of the TRα1 receptor: Consequences of LT4 treatment. J Clin Endocrinol Metab 2013;98(7): 3029–3038; doi: 10.1210/jc.2013-1050
7. O'Shea PJ, Bassett JH, Sriskantharajah S, et al. Contrasting skeletal phenotypes in mice with an identical mutation targeted to thyroid hormone receptor alpha1 or beta. Mol Endocrinol 2005;19(12):3045–3059; doi: 10.1210/me.2005-0224
8. O'Shea PJ, Bassett JH, Cheng SY, et al. Characterization of skeletal phenotypes of TRalpha1 and TRbeta mutant mice: Implications for tissue thyroid status and T3 target gene expression. Nucl Recept Signal 2006;4:e011; doi: 10.1621/nrs.04011
9. Bassett JH, Boyde A, Zikmund T, et al. Thyroid hormone receptor α mutation causes a severe and thyroxine-resistant skeletal dysplasia in female mice. Endocrinology 2014; 155(9):3699–3712; doi: 10.1210/en.2013-2156
10. Park S, Han CR, Park JW, et al. Defective erythropoiesis caused by mutations of the thyroid hormone receptor α gene. PLoS Genet 2017;13(9):e1006991; doi: 10.1371/journal.pgen.1006991
11. Han CR, Park S, Cheng SY. NCOR1 modulates erythroid disorders caused by mutations of thyroid hormone receptor α1. Sci Rep 2017;7(1):18080; doi: 10.1038/s41598-017-18409-4
12. Bao L, Roediger J, Park S, et al. Thyroid hormone receptor alpha mutations lead to epithelial defects in the adult intestine in a mouse model of resistance to thyroid hormone. Thyroid 2019;29(3):439–448; doi: 10.1089/thy.2018.0340
13. Kaneshige M, Suzuki H, Kaneshige K, et al. A targeted dominant negative mutation of the thyroid hormone alpha 1 receptor causes increased mortality, infertility, and dwarfism in mice. Proc Natl Acad Sci U S A 2001;98(26):15095–15100; doi: 10.1073/pnas.261565798
14. Han CR, Wang H, Hoffmann V, et al. Thyroid hormone receptor α mutations cause heart defects in zebrafish. Thyroid 2021;31(2):315–326; doi: 10.1089/thy.2020.0332
15. May AT, Crowe MS, Blakeney BA, et al. Identification of expression and function of the glucagon-like peptide-1 receptor in colonic smooth muscle. Peptides 2019;112:48–55; doi: 10.1016/j.peptides.2018.11.007
16. Alberto AV, Bonavita AG, Fidalgo-Neto AA, et al. Single-cell microinjection for cell communication analysis. J Vis Exp 2017;120:50836; doi: 10.3791/50836
17. Stringer C, Pachitariu M. Cellpose 2.0: how to train your own model. BioRxiv 2022;1–14; doi: 10.1101/2022.04.01.486764
18. Maier F, Siri S, Santos S, et al. The heterogeneous morphology of networked collagen in distal colon and rectum of mice quantified via nonlinear microscopy. J Mech Behav Biomed Mater 2021;113:104116; doi: 10.1016/j.jmbbm.2020.104116
19. Evans WH, Martin PE. Gap junctions: Structure and function (review). Mol Membr Biol 2002;19(2):121–136; doi: 10.1080/09687680210139839
20. Stauch K, Kieken F, Sorgen P. Characterization of the structure and intermolecular interactions between the con-

nexin 32 carboxyl-terminal domain and the protein partners synapse-associated protein 97 and calmodulin. J Biol Chem 2012;287(33):27771–27788; doi: 10.1074/jbc.M112.382572
21. Li H, Spagnol G, Naslavsky N, et al. TC-PTP directly interacts with connexin43 to regulate gap junction intercellular communication. J Cell Sci 2014;127(Pt 15):3269–3279; doi: 10.1242/jcs.145193
22. Green LM, LaBue M, Lazarus JP, et al. Reduced cell-cell communication in experimentally induced autoimmune thyroid disease. Endocrinology 1996;137(7):2823–2832; doi: 10.1210/endo.137.7.8770903
23. Hanani M. Lucifer yellow—an angel rather than the devil. J Cell Mol Med 2012;16(1):22–31; doi: 10.1111/j.1582-4934.2011.01378.x
24. Fukata Y, Amano M, Kaibuchi K. Rho-Rho-kinase pathway in smooth muscle contraction and cytoskeletal reorganization of non-muscle cells. Trends Pharmacol Sci 2001;22(1):32–39; doi: 10.1016/s0165-6147(00)01596-0
25. Sanders KM, Koh SD, Ro S, et al. Regulation of gastrointestinal motility-insights from smooth muscle biology. Nat Rev Gastroenterol Hepatol 2012;9(11):633–645; doi: 10.1038/nrgastro.2012.168
26. Lennartsson J, Jelacic T, Linnekin D, et al. Normal and oncogenic forms of the receptor tyrosine kinase kit. Stem Cells 2005;23(1):16–43; doi: 10.1634/stemcells.2004-0117
27. Iino S, Horiguchi S, Horiguchi K, et al. Interstitial cells of Cajal in W(sh)/W(sh) c-kit mutant mice. J Smooth Muscle Res 2020;56(0):58–68; doi: 10.1540/jsmr.56.58
28. Morimoto M. Intestinal smooth muscle cells locally enhance stem cell factor (SCF) production against gastrointestinal nematode infections. J Vet Med Sci 2011;73(6):805–807; doi: 10.1292/jvms.10-0548
29. Shafer RB, Prentiss RA, Bond JH. Gastrointestinal transit in thyroid disease. Gastroenterology 1984;86(5 Pt 1):852–855.
30. Plateroti M, Chassande O, Fraichard A, et al. Involvement of T3Ralpha- and beta-receptor subtypes in mediation of T3 functions during postnatal murine intestinal development. Gastroenterology 1999;116(6):1367–1378; doi: 10.1016/s0016-5085(99)70501-9
31. Gauthier K, Chassande O, Plateroti M, et al. Different functions for the thyroid hormone receptors TRalpha and TRbeta in the control of thyroid hormone production and post-natal development. EMBO J 1999;18(3):623–631; doi: 10.1093/emboj/18.3.623

Address correspondence to:
Sheue-yann Cheng, PhD
Gene Regulation Section
Laboratory of Molecular Biology
National Cancer Institute
National Institutes of Health
37 Convent Door, Room 5128
Bethesda, MD 20892-4264
USA

E-mail: chengs@mail.nih.gov